Clutter Effect on the Miss Distance of a Radar Homing Missile

Susumu Miwa*
Tokyo Denki University, Tokyo, Japan
and
Fumiaki Imado† and Takeshi Kuroda‡
Mitsubishi Electric Corporation, Tokyo, Japan

When the target Doppler frequency in a radar homing missile crosses the main lobe clutter spectrum at the terminal phase of its flight, a large miss distance is induced. This paper presents the quantitative analysis on this clutter effect using a program named SAMS (Statistical Assessment of Missile Systems), which is a hierarchical and generalized version of the SLAM (Statistical Linearization Adjoint Method). A homing missile is represented by triple time constants, a limiter, a second-order missile airframe, and proportional navigation. The main lobe clutter is imposed on to this system along with the target random maneuver, glint, fading, and receiver noise. By processing the covariance propagation of the system equation and the adjoint system, the miss distance and the contribution of each noise are calculated. The results reveal that the clutter effect is maximized if the target Doppler frequency begins to cross the main lobe clutter spectrum 2 s prior to the terminal time, and it is largely enhanced if the target random maneuver is combined. These effects are reduced, however, if the missile lateral acceleration capability is increased or the target lateral acceleration decreased. The radome effect is also analyzed by adding the related feedforward loop to the original system, which makes a considerable change in the miss distance.

Nomenclature

$A(s)$	= missile airframe transfer function
B	= target lateral acceleration
C	= received clutter power
$G(t)$	= clutter imposition function
h^*	= impulse response of adjoint system
K_{eq}	= equivalent gain of limiter
k_m	= antenna-type dependent coefficient
Lim	= limiter level of missile lateral acceleration command
MD	= miss distance = $\sigma(t_f)$
N	= noise power
n_{eff}	= effective navigation constant
R_{TM}	= range between missile and target
RS	= radome bore-sight error slope
S	= received signal power
T	= noise correlation time
T_A, T_H	= autopilot and homing head time constants, respectively
T_N	= noise filter time constant
t	= time
t_f	= final time
v_c	= closing velocity
x	= state variable
θ_R	= receiver antenna beamwidth
λ	= state variable of adjoint system
$2v$	= target maneuver bandwidth
Φ	= noise power spectral density
$\sigma(t)$	= standard deviation distance at time t
τ_α	= missile incidence lag
$(\ )_{CN}$	= clutter
$(\ )_{FN}$	= fading noise
$(\ )_{GN}$	= glint noise
$(\ )_{RN}$	= receiver noise
$(\ )_{TN}$	= target random maneuver

Received June 1 1987; presented as Paper 87-2449 at the AIAA Guidance, Navigation and Control Conference, Monterey, CA, Aug. 17–19, 1987; revision received Oct. 1, 1987.

*Professor, Faculty of Engineering.
†Chief Engineer, Mechanical Systems and Technology Department, Central Research Laboratory. Member AIAA.
‡Engineer, Central Research Laboratory.

Introduction

IN a radar homing missile, the target Doppler frequency coincides with the main lobe clutter when the target velocity vector comes close to perpendicular to the line of sight (LOS) and, in the case of lookdown, the level of the main lobe clutter far exceeds the target signal. It is therefore easily assumed that if the target maneuvers with a large lateral acceleration at low altitude, it may have a chance to be masked by the main lobe clutter. The missile seeker angle, as well as the rudder command signal, is largely contaminated at this period. The miss distance may be adversely affected if the target crosses the main lobe clutter at the terminal phase because it has insufficient time to recover from the disturbance.

We analyzed the situation and showed that the missile initial positions at which this effect occurs form a pair of spiral zones and that the spiral turning rate depends on the target speed and lateral acceleration.[1] However, the quantitative analysis of the main lobe clutter effect was not included in our analysis. It may be more convincing if the miss distance caused by the clutter is calculated and compared with other noise sources.

The Statistical Linearization Adjoint Method (SLAM),[2] an approach for the complete statistical analysis of a nonlinear missile guidance system through the combination of the CADET method[3] and the adjoint technique, proved to be an excellent design and analysis tool for missile guidance systems. This method was applied to a triple time-constant nonlinear kinematic guidance loop, with random target maneuver, glint, and fading added as noise sources, and showed the miss distance budget as a function of missile acceleration limits. This method was applied to give more detailed analyses of noise[4] and radome effects,[5] though analyses were done using linear systems.

We found this method so useful that we produced a more hierarchy-oriented and generalized version of it, named SAMS (Statistical Assessment of Missile Systems).[6] The SAMS program made it easier to calculate the noise effect, including the main lobe clutter effect, against various types of missile block diagrams.

In this paper, features of the SAMS program are introduced first. Second, the block diagrams of semiactive radar homing missiles, and the kinds and values of the noise added to the system, are explained. Third, simulation results are shown. After checking the compatibility of these results with the results of SLAM, the effect of the main lobe clutter is shown as a function of the time at which the main lobe clutter starts to cover the target signal. Further, the effect of the target random maneuver combined with the clutter is checked. Also shown are the MD's when the missile lateral acceleration command limit and the target lateral acceleration level are changed and the radome effect is added.

The SAMS Program

In this section, features of the SAMS program are explained after a brief review of SLAM.

The Statistical Linearization Adjoint Method, beautifully developed by P. Zarchan, is an exceptionally promising technique for the complete statistical analysis of nonlinear homing missile guidance systems.

The principal steps in the SLAM system generation are:

1) Replace each nonlinear element in the original system with its corresponding random input describing function gain, based on an assumed Gaussian probability density function for the input to the nonlinearity.

2) Describe the linearized system function, and employ conventional covariance analysis techniques to propagate the statistics of the system state vector.

Processes 1 and 2 are called CADET.

3) Store the resulting describing function gain for each nonlinearity as a function of time.

4) Generate an adjoint model of the linearized system model by replacing t with $t_f - t$ in the argument of all variable coefficients (including describing function gains) and using signal flow so that the inputs of the original system appear as outputs of the adjoint system.

The Statistical Assessment of Missile Systems is developed to give more flexibility and generality to be applied with various types of missile systems. The main differences between SAMS and SLAM lie in steps 2 and 4.

In step 2 in SAMS, a system matrix is directly composed in a computer by inputting the system block diagram. To perform this, a hierarchical program structure is adopted. The fundamental block diagram of a missile system is given in Fig. 1, where each block is called a "function unit." Each function unit consists of four types of "fundamental elements," namely, a gain, an addition, an integration, and a nonlinear element.

A combination of a new fundamental element with an existing unit generates a renewed system matrix. As any combination can be categorized into limited numbers of types, this generation can be automatically processed in the computer.[7]

What a user of this program must do is to describe a block diagram of each function unit using the four fundamental elements and designate line numbers between the connected elements. A modification of the unit is performed by an addition, a deletion, or a combination change of fundamental elements. If variable types of function units are prepared, different systems are easily composed by merely changing the units.

Generally a linear time-varying system is expressed by Eq. (1), whereas its adjoint system is defined by Eq. (2).

$$x' = F(t)x \tag{1}$$

$$\lambda' = -F^T(t)\lambda \tag{2}$$

The impulse response of the adjoint system gives the relation between the output (MD) and input (noise power density) according to Eq. (3), which gives the contribution of each input noise to the miss distance.

$$(\mathrm{MD})^2 = \int_0^{t_f} \Phi_{\mathrm{in}}[h^*(\tau)]^2 \, \mathrm{d}\tau \tag{3}$$

In step 4 in SAMS, the adjoint system is also directly produced according to its definition, instead of replacing t with $t_f - t$ and reversing the signal flow as in SLAM.

The flow diagram of SAMS is shown in Fig. 2, where biased inputs at an arbitrary period of time can also be handled.

The scale of the SAMS program (approximately 10,000 steps in FORTRAN) may be considerably larger compared with that of SLAM because of its hierarchical structure; however, its flexibility and ease of operation pay off when the results for different block diagrams are required.

Simulation Model

The system block diagram and the noise inputs used in the simulation are shown in Fig. 3. Calculations are made mainly by using the loop, indicated by bold arrowed lines, which comprises triple time constants, a limiter, a second-order missile airframe, and the proportional navigation. This model is defined here as a "standard model." If the missile airframe block is removed, the system is equivalent to the model used in SLAM, though nominal values are slightly different. The thin arrowed lines are added when the radome effect is analyzed.

The receiver noise and clutter are added to the system, along with the target random maneuver, glint, and fading. Both the receiver noise and clutter have standard deviation angles proportional to R_{TM}, whereas the glint gives an angle inversely proportional to R_{TM}, and the angle due to fading is indifferent to R_{TM}.

The clutter is assumed to last for 1 s, judging from the previous analysis of the clutter and the target power spectra.[1] Four cases are considered for the clutter starting time, namely $t_f - 4$, $t_f - 3$, $t_f - 2$, and $t_f - 1$ s, in order to analyze its effect.

The standard deviation angle of the seeker caused by various noise sources with relation to R_{TM} is summarized in Fig. 4.

The nominal values of all system parameters used are tabulated in Table 1.

Comments on some items in Table 1 are:

1) Values of R_{TM}, v_c are obtained for the following simulation. A point mass target turns with a constant lateral acceleration as soon as a typical air-to-air missile is fired at a head-on position. Changing the initial range enables the trajectories to be found where the target Doppler frequency begins to cross the main lobe clutter at $t_f - 4$, $t_f - 3$, $t_f - 2$, and $t_f - 1$ s.

2) The standard deviation angle caused by the receiver noise

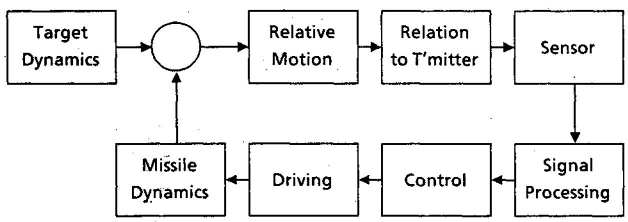

Fig. 1 Function units in SAMS program.

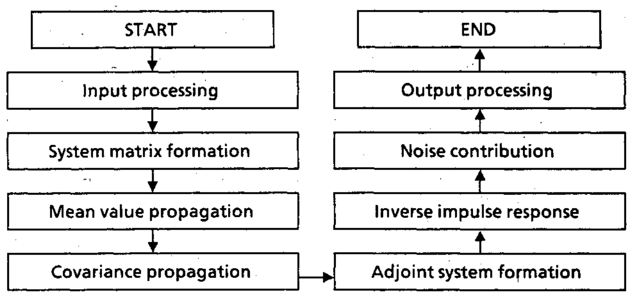

Fig. 2 Flow diagram of SAMS program.

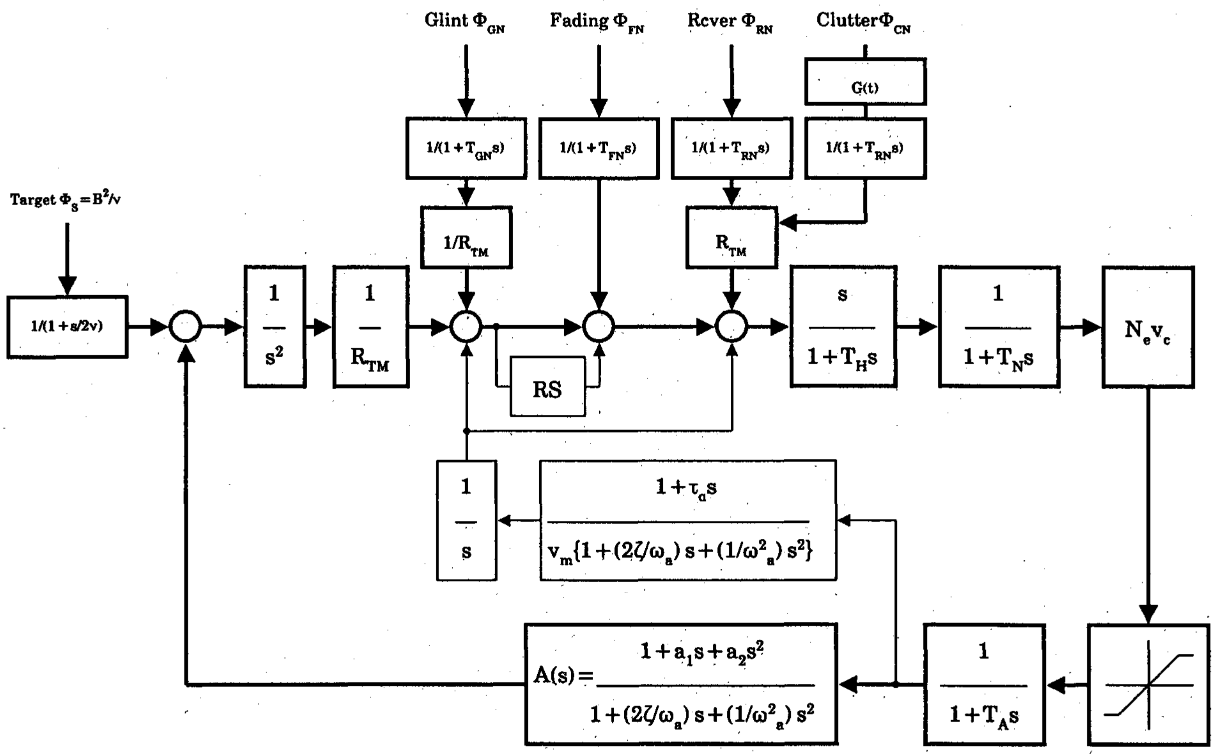

Fig. 3 System block diagram.

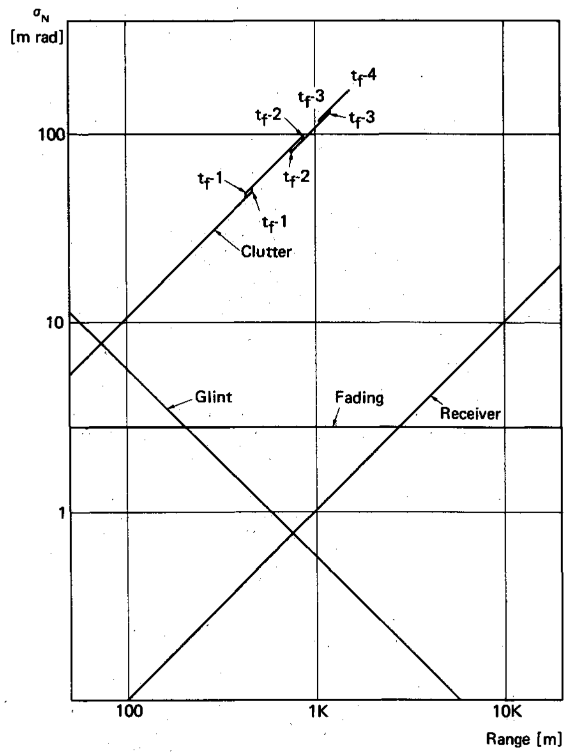

Fig. 4 Standard deviation angle caused by various noises.

Table 1 Nominal values of all system parameters

Symbol	Nominal value	Unit
T_H	0.05	s
T_N	0.15	s
T_A	0.1	s
$A(s)$	$\dfrac{1+0.001s^2}{1+(2\times 0.7/20)s+(1/20^2)s^2}$	
Lim	30 unless specified	G
$2v$	0.2	1/s
B	5 unless specified	G
$G(t)$	1 for clutter time of 1 s 0 for remaining	
R_{TH}, v_c,	See comment (1) regarding this table	
t_f	8.0	s
N_e	3	
Φ_{GN}	6.3×10^{-7}	rad²/Hz at 1 km
T_{GN}	0.05	s
Φ_{FN}	1×10^{-6}	rad²/Hz
T_{FN}	0.01	s
Φ_{RN}	1.26×10^{-7}	rad²/Hz at 1 km
T_{RN}	0.01	s
Φ_{CN}	1.47×10^{-3}	rad²/Hz at 1 km
T_{CN}	0.01	s
RS	0.05	deg/deg
τ_α	2	s

is selected as 1 mil-rad at $R_{TM} = 1$ km, which gives a receiver S/N ratio of 40 dB.

3) The main lobe clutter power is in the order of -60 dBm/kHz. The signal power comes to approximately the same level at $R_{TM} = 1$ km. The standard deviation angle caused by the clutter becomes 0.108 rad by using Eq. (4), where $\theta_R = 13$ deg, $k_m = 1.5$, and $S/C = 0$ dB.

$$\sigma_{CN} = \theta_R \bigg/ \left(k_m \sqrt{\frac{2S}{C}}\right) \tag{4}$$

4) Equation (5) expresses the relation among the power spectral density, correlation time, and standard deviation.

$$\Phi_N = 2T_N\sigma_N^2 \tag{5}$$

Simulation Results

Simulations are conducted for six cases using the standard model. The limiter level and the target lateral acceleration are assumed to be 30 and 5 G, respectively, unless otherwise specified.

Case 1: With Target Maneuver, Without Clutter

First, the target random maneuver, glint, and receiver noise are imposed. Propagation of $\sigma(t)$ is shown in Fig. 5. The $\sigma(t)$ value increases with time up to about 5 s, then decreases toward the final time. The $\sigma(t_f)$ value, which is the MD, is 8.7 m.

The model used in Ref. 2 (SLAM) is formed by deleting the missile airframe transfer function and the receiver noise input from the standard and slightly changing the T_N value. The MD of 5.4 m is obtained using this model calculated by SAMS, which naturally coincides with the result in Ref. 2. Further analysis made it clear that this MD difference (8.7 vs 5.4 m) is caused mainly by the airframe.

Figure 6 shows the equivalent gain K_{eq} of the limiter, which is a prime nonlinear element in this model. The value is nearly equal to unity from the start to approximately 7 s, then rapidly decreases to 0.2 at t_f. This decrease is due to saturation of the limiter by noises.

Contributions of various noises to MD against the adjoint time $t_f - t$ are plotted in Fig. 7. The value at $t_f - t = t_f$ represents the contribution of each noise to MD. They are 8.1 m by target random maneuver, 2.9 m by glint, 0.8 m by fading, and 0.2 m by receiver. The MD caused by the target is not negligible.

Case 2: Without Target Maneuver, With Clutter

Second, the target is not assumed to maneuver randomly, but the clutter noise is imposed at $t_f - 4$, $t_f - 3$, $t_f - 2$, and $t_f - 1$ s for 1 s. The propagation of $\sigma(t)$ is shown in Fig. 8. If the clutter is applied at $t_f - 4$ s, a sharp increase occurs and the maximum value of $\sigma(t)$ becomes approximately 28 m at 6.5 s, then decreases thereafter to 3.0 m at t_f. If applied at $t_f - 3$ s, $\sigma(t)$ at maximum and the MD are 16 and 3.7 m, respectively. The later the clutter is imposed, the smaller the maximum value of $\sigma(t)$ becomes. This is due to the assumption that the clutter is proportional to R_{TM}. In the case of $t_f - 2$ s, the MD becomes nearly equal to the maximum $\sigma(t)$, which is 8.9 m. In the case of $t_f - 1$ s, $\sigma(t)$ has insufficient time to develop, resulting in 4.3-m MD.

Figure 9 shows K_{eq} values. The effect of the clutter is clearly shown by the suppressed gain during the period of clutter.

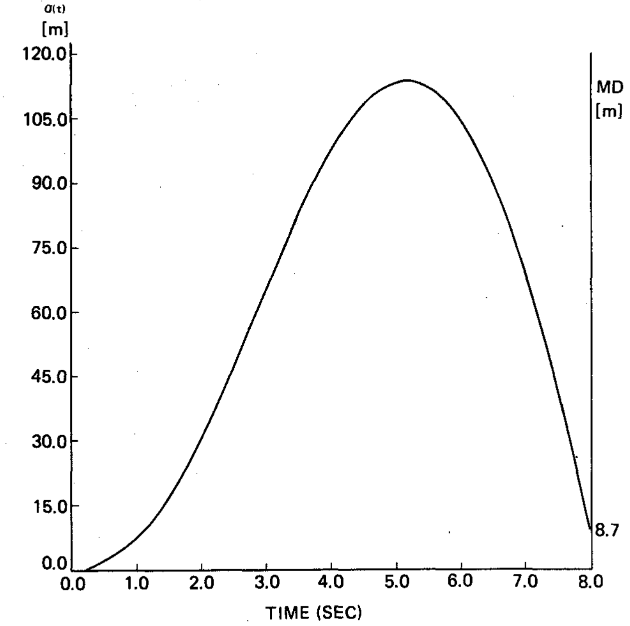

Fig. 5 $\sigma(t)$ **for "with target maneuver, without clutter."**

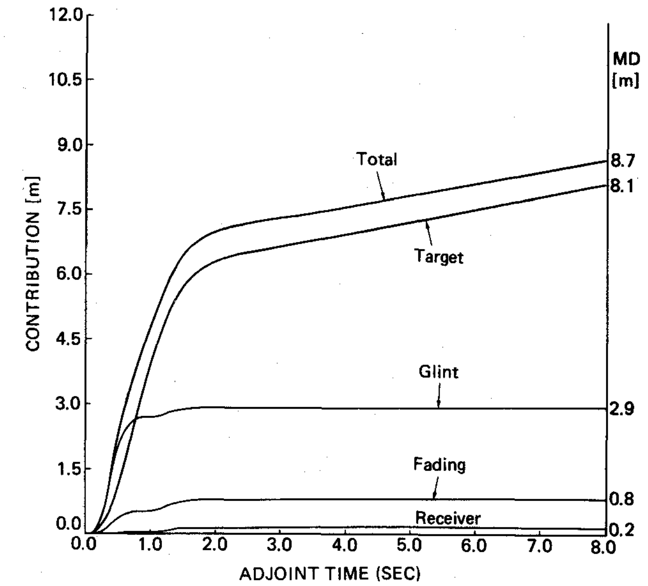

Fig. 7 Noise contribution for "with target maneuver, without clutter."

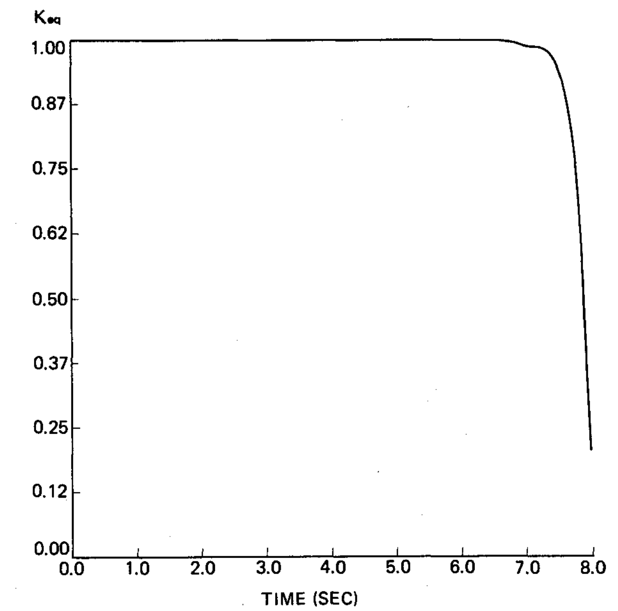

Fig. 6 K_{eq} **for "with target maneuver, without clutter."**

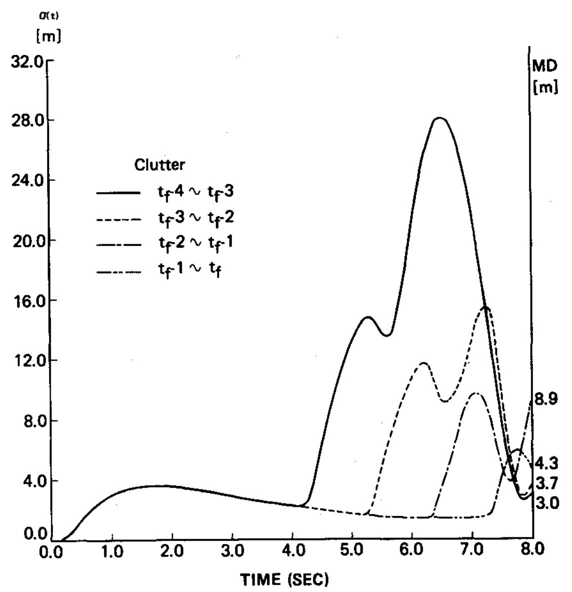

Fig. 8 $\sigma(t)$ **for "without target maneuver, with clutter."**

The contributions of various noises to MD are summarized in Table 2.

It is concluded that the clutter gives a considerably large MD if it is applied at $t_f - 2$ s, but not large enough to be considered detrimental to the system.

Case 3: With Target Maneuver and Clutter

In this situation, the target makes random maneuvers during which the target Doppler frequency crosses the main lobe clutter. The propagation of $\sigma(t)$ is shown in Fig. 10. When the clutter is applied at $t_f - 4$ s, its maximum value reaches 150 m and the MD becomes 11.5 m. In the case of $t_f - 2$ s, the MD increases to 32.2 m, while in the $t_f - 1$ s case, it decreases again to 16.9 m. The MD's in this situation far exceed those in cases 1 and 2; in other words, a combination of the target random maneuver and clutter largely enhances the MD caused by the target or clutter alone.

The contributions of various noises to MD are summarized in Table 3.

Judging from Table 3, the target random maneuver contributes most to MD; however, this is interpreted as being caused by the combination of the target maneuver and the suppressed nonlinear equivalent gain by the clutter.

Case 4: Effect of the Limit Level

The lateral acceleration command limit of the missile is set at 30 G so far. If this limit were allowed to be higher, a smaller MD would be expected. Simulations are conducted by changing the level to 20 and 40 G. Results are shown by the solid lines in Fig. 11.

In the case of "with target maneuver, without clutter," which corresponds to case 1, the MD for 20 G is 12.6 m, which is larger than 8.7 m for 30 G, and the target maneuver still has the dominant effect, sharing in 12.3 m of the MD. For 40 G, the MD equals 8.0 m, and the target contribution comes to 7.5 m.

In the case of "with target maneuver and clutter," which corresponds to case 3, the maximum MD appears when the clutter is added at $t_f - 2$ s. Therefore, the results are plotted only for this condition. The MD of 32.2 m for 30 G changes to 62.8 and 17 m for 20 and 40 G, respectively. The combination

Table 2 Noise contribution to MD in case 2

Clutter time, s	Clutter, m	Glint, m	Fading, m	Receiver, m	Total, m
$t_f - 4$	1.2	2.7	0.5	0.1	3.0
$t_f - 3$	2.5	2.7	0.6	0.1	3.7
$t_f - 2$	8.4	3.0	0.7	0.1	8.9
$t_f - 1$	3.6	2.2	0.6	0.2	4.3

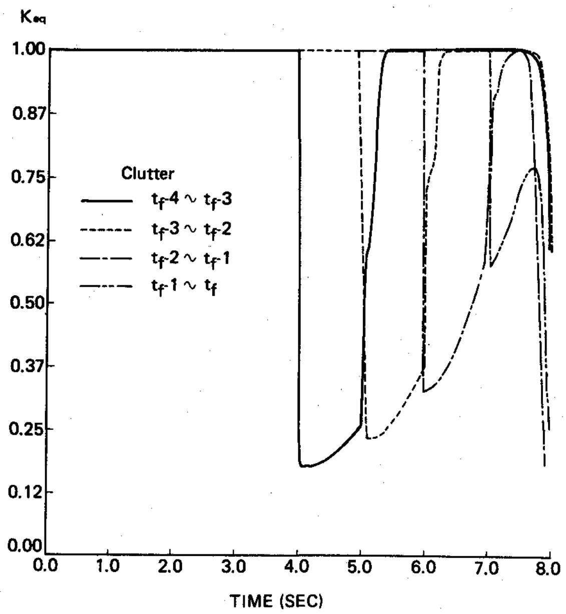

Fig. 9 K_{eq} for "without target maneuver, with clutter."

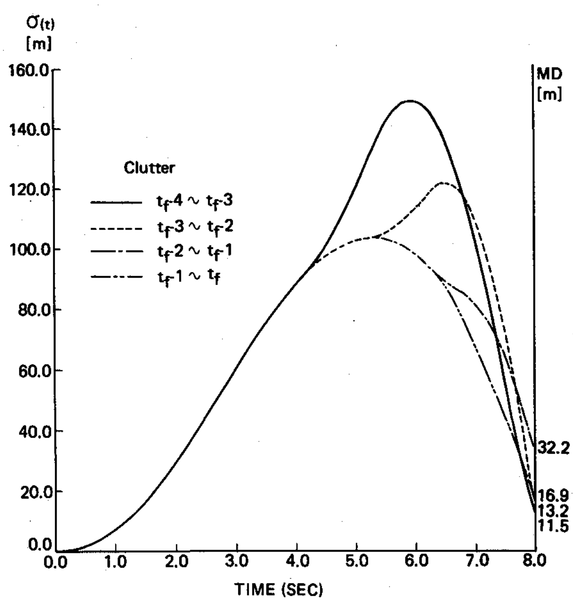

Fig. 10 $\sigma(t)$ for "with target maneuver and clutter."

Table 3 Noise contribution to MD in case 3

Clutter time, s	Clutter, m	Glint, m	Fading, m	Receiver, m	Target, m	Total, m
$t_f - 4$	1.5	2.7	0.5	0.1	11.1	11.5
$t_f - 3$	1.0	2.4	0.5	0.1	13.0	13.2
$t_f - 2$	5.8	2.1	0.6	0.2	31.6	32.2
$t_f - 1$	4.1	2.2	0.7	0.2	16.2	16.9

Table 4 Noise contribution to MD in case 4

Missile acc., G	Clutter $t_f - 2$ s	Glint, m	Fading, m	Receiver, m	Target, m	Total, m
20	3.3	2.2	1.5	0.6	62.6	62.8
30	5.8	2.1	0.6	0.2	31.6	32.2
40	7.9	2.5	0.6	0.1	14.8	17.0

Table 5 Noise contribution to MD in case 5

Target acc., G	Missile acc., G	Clutter, m	Glint, m	Fading, m	Receiver, m	Target, m	Total, m
3	20	5.1	2.2	1.0	0.4	25.2	25.9
3	30	7.5	2.6	0.6	0.1	10.0	12.7
3	40	8.6	2.8	0.6	0.1	5.4	10.3
7	20	3.5	2.2	1.7	0.7	112.3	112.4
7	30	4.1	1.9	0.9	0.3	63.3	63.4
7	40	6.8	2.2	0.6	0.1	33.8	34.5

Table 6 Noise contribution to MD in case 6

Missile acc., G	Clutter, m	Glint, m	Fading, m	Receiver, m	Target, m	Total, m
20	—	2.0	0.6	0.2	19.9	20.0
30	—	2.1	0.5	0.2	11.9	12.1
40	—	2.2	0.5	0.1	10.3	10.5
20	2.9	1.8	1.2	0.5	73.0	73.1
30	3.5	1.9	0.6	0.2	39.3	39.5
40	4.8	2.1	0.4	0.1	21.8	22.4

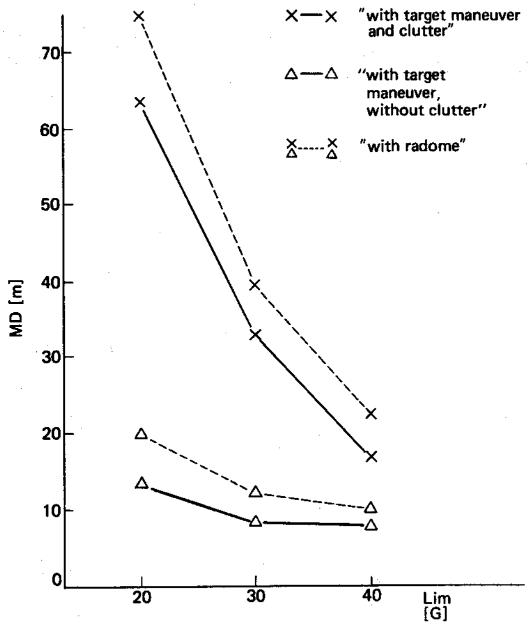

Fig. 11 Effect of missile lateral acceleration limit and radome.

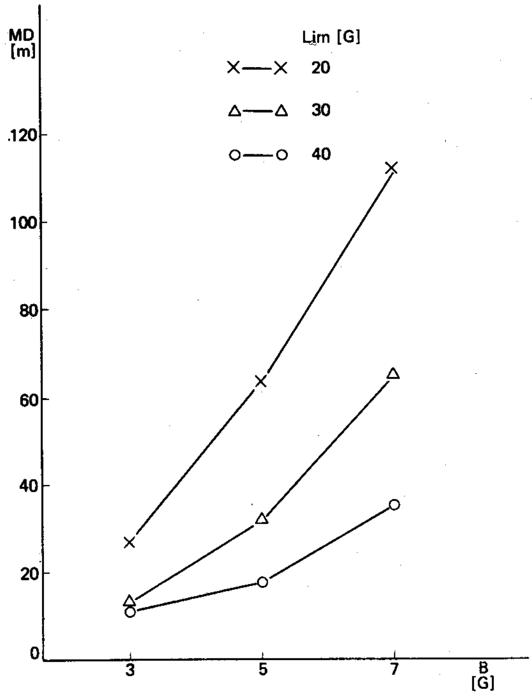

Fig. 12 Effect of target lateral acceleration.

effect of target maneuvers and clutter cannot be overlooked, even for a missile having a 40-G limit.

The contributions of various noises to MD in the latter case are summarized in Table 4.

Case 5: Effect of Target Lateral Acceleration

As the target random maneuver is dominant in the MD contribution, it is expected that the value of B will influence MD. The MD is plotted against B in Fig. 12 for the limiter level as a parameter. If B is 3 G, the MD's are 25.9, 12.7, and 10.3 m for the limiter levels of 20, 30, and 40 G, respectively, whereas, if B takes a 7 G maneuver, the MD's become 112.4, 63.4, and 34.5 m.

The noise contributions to MD are summarized in Table 5.

Case 6: Effect of Radome Slope

In order to introduce the radome bore-sight error slope into the system, another feedforward loop must be added as shown by the thin arrowed lines in Fig. 3. This complicated model is also easily processed by SAMS, resulting in about 30-s run time with a 5-MFLOPS class computer.

The results corresponding to case 4 are shown in Fig. 11 with dotted lines. The lower line indicates the case for "without clutter" and the upper line is for "with clutter" at $t_f - 2$ s. The difference between the solid and dotted lines is caused by the radome slope, which lies between 2.5 and 7.4 m in the former, case, and 5.4 to 10.3 m in the latter case, depending on the limiter level. It can be said that the radome slope influences the MD considerably, especially if the clutter is imposed.

The noise contributions to MD are summarized in Table 6.

Conclusions

The SAMS program, the hierarchical and generalized version of the SLAM, makes it possible to calculate the miss distance and the noise contribution to the miss distance by simple input systems for a computer.

Simulations are conducted against a semiactive radar homing system, with noise inputs such as the target random maneuver and clutter added. The results for the standard model show the following:

1) In the case of "with target maneuver, without clutter," the miss distance becomes 8.7 m, and the target maneuver is a major contributor to the miss distance.

2) In the case of "without target maneuver, with clutter," the miss distance changes according to the clutter starting time. The maximum miss distance, which is 8.9 m, occurs when the target Doppler frequency begins to cross the main lobe clutter at 2 s prior to intercept.

3) If both target maneuver and clutter are applied, the miss distance is greatly enhanced to 32.2 m for the clutter starting time of 2 s prior to intercept. This is caused by the combined effect of the target maneuver and the suppressed limiter gain caused by the clutter.

4) The larger the increase in the missile acceleration command limit, the smaller the miss distance becomes. The 32.2 m cited for the 30-G limit changes to 62.8 m for 20 G and 17.0 m for 40 G.

5) If the target acceleration increases, the miss distance increase sharply, with the 32.2 m for 5 G increasing to 63.4 m at 7 G and decreasing to 12.7 m at 3 G. The same relation holds for the 20- and 40-G limit.

6) The radome slope effect is obtained by adding the radome bore-sight error slope and another feedforward loop to the standard. The 0.05 deg/deg error slope yields a 2.5–10.3-m miss distance increase, depending on the limiter level and clutter.

Acknowledgments

The authors are indebted to Prof. M. Higashiguchi and Prof. K. Kato of Tokyo University for their guidance and to Mr. T. Nishimura of Mitsubishi Research Institute for the cooperation in developing the SAMS program.

References

[1]Miwa, M. and Imado, F., "Clutter Effect on the Guidance of a Semi-Active Radar Homing Missile," *Journal of Guidance, Control, and Dynamics*, Vol. 9, May–June 1986, pp. 268–273.

[2]Zarchan, P., "Complete Statistical Analysis of Nonlinear Missile Guidance System-SLAM," *Journal of Guidance and Control*, Vol. 2, Jan.–Feb. 1979, pp. 71–78.

[3]Gelb, A. and Warren, R. S., "Direct Statistical Analysis of Nonlinear Systems: CADET," *AIAA Journal*, Vol. 11, May 1973, pp. 689–694.

[4]Nesline, F. W. and Zarchan, P., "Miss Distance Dynamics in Homing Missiles," AIAA Paper 84-1854, Aug. 1984.

[5]Nesline, F. W. and Zarchan, P., "Radome Induced Miss Distance in Aerodynamically Controlled Homing Missiles," AIAA Paper 84-1855, Aug. 1984.

[6]Imado, F., Miwa, S., and Nishimura, T., "Statistical Assessment Program of Missile Systems-SAMS, Part 1. General Description," *Proceedings of the JSAAS Aircraft Symposium*, Japan Society for Aeronautical and Space Sciences, Tokyo, Oct. 1985 (in Japanese).

[7]Nishimura, T., Imado, F., and Miwa, S., "Statistical Assessment Program of Missile Systems-SAMS, Part 2. Algorithm for System Matrix Development," *Proceedings of the JSASS Aircraft Symposium*, Japan Society for Aeronautical and Space Sciences, Tokyo, Oct. 1985 (in Japanese).